Vol. 186: 87–93, 1999 | MARINE ECOLOGY PROGRESS SERIES
Mar Ecol Prog Ser | Published September 17

The importance of ciliates for interstitial solute transport in benthic communities

Ronnie Nøhr Glud*, Tom Fenchel

Marine Biological Laboratory, University of Copenhagen, Strandpromenaden 5, 3000 Helsingør, Denmark

ABSTRACT: By 3 different approaches we demonstrate the ability of filter feeding ciliates (*Euplotes* spp. and *Uronema marinum*) to enhance interstitial solute transports. By a simple diffusion analogy we quantify the effect as a function of cell densities. Ciliate densities often encountered in biofilms, microbial mats or estuarine sediments may enhance the transport coefficients of biogeochemical important solutes like, for instance, O_2 by a factor of 1.1 to 10 above the diffusive coefficient. In less productive environments (coastal or shelf sediments) ciliate densities are usually too low to cause any significant effect on the diffusive mediated solute transport, at least in the case of small fast-diffusing molecules such as O_2.

KEY WORDS: Diffusion · Solutes · Ciliates · Dispersion · Porewater · Transport coefficients

INTRODUCTION

The sediment water interface is a highly active zone of the marine environment, typically characterized by steep concentration gradients of dissolved solutes. It is generally assumed that solute transport in sediments and across the benthic interface is mediated by molecular diffusion (e.g. Boudreau 1997). Bioirrigation may add significantly to surficial solute transport in sediments inhabited by macrofauna (e.g. Archer & Devol 1992) and a special case of convective solute transport induced by veil-forming sulphide-oxidizing bacteria has recently been demonstrated (Fenchel & Glud 1998). Despite occasional speculation on the importance of meio- and microfauna for benthic solute transport, only a few studies quantifying such effects have been performed. Aller & Aller (1992) showed that natural densities of meiofauna could stimulate solute transport in interstitial water by a factor of 1.7 to 2.3 over diffusion. About 30% of this effect was ascribed to increased porosity, while the rest was caused by interstitial water mixing induced mainly by nematodes, juvenile bivalves and polychaete larvae. Microsensor studies of a microbial mat have also demonstrated a 20% decrease in solute transport after poisoning of the community and the observation was mainly ascribed to inhibition of meiofaunal activity (Glud et al. 1995).

Protozoa account for a significant fraction of the interstitial microbiota, but to our knowledge no effort has so far been dedicated to investigations on their importance for solute transport. Among protozoa, the most likely candidates to stimulate non-diffusive solute transport are filter feeding ciliates. It has been shown that commonly occurring interstitial ciliates like *Uronema* spp. and *Euplotes* spp. have a volume specific clearance on the order of 10^5 h^{-1}, which corresponds to an approximate filtration rate of 6 to 50 µl d^{-1} (Fenchel 1986). In benthic communities with high densities of filter feeding ciliates, such activity could potentially be of importance for interstitial solute transport. We have investigated to which extent ciliates (*Euplotes* spp. and *U. marinum*) stimulate the benthic solute transport and the results are discussed in the context of solute dynamics in naturally occurring marine sediments.

MATERIALS AND METHODS

Ciliates. Sediment samples were collected from Nivå Bay (25 km north of Copenhagen, Denmark). In the

*E-mail: mblrg@mail.centrum.dk

laboratory individuals of *Euplotes vannus*, *E. moebiusi*, *E. charon* and *Uronema marinum* were isolated and maintained in Nunclon tissue culture flasks containing seawater (salinity 20‰) with wheat grains (1 to 2 boiled wheat grains per 100 ml of seawater). When large numbers of ciliates were required, cells were grown in suspensions of bacteria in sterile seawater (*U. marinum*) or in suspensions of *Rhodomonas* or yeast cells (*Euplotes* spp.). In some cases the cell density was further increased by centrifugation and/or filtration prior to experiments. The cell volume of the *Euplotes* species was about 2×10^4 µm^3, while the typical size of *U. marinum* was about 3×10^3 µm^3. Experimental data showed no difference between the 3 species of *Euplotes* investigated and in the following discussion we have not distinguished between them.

Empirical model. We approached any ciliate stimulate solute transport by a simple empirical model. Here, each individual ciliate was treated as a pump sitting in a homogenous medium. From measured flow velocity vectors around individual cells the flow field surrounding a ciliate was approximated (see below). The transport of solutes between evenly spaced, randomly oriented cells was subsequently approached as 'random walk'.

In order to determine the flow lines around ciliates, Teflon spheres were added to suspensions of cells. Flow velocity vectors around swimming and stationary (filter feeding) cells were then quantified from the displacement of individual Teflon spheres as recorded by a CCD video camera (Sony DXC 101P) mounted on a microscope (Fenchel 1986). As expected for motion at low Renoylds numbers (Purcell 1977), swimming ciliates caused only marginal mixing of added Teflon spheres (Fig. 1A). In contrast to this, stationary and feeding individuals created a flow field reaching maximum flow velocities of 0.6 to 1.2 mm s^{-1} close to the mouth (Fig. 1B). By defining the individual ciliate as a point placed at (0,0) of a Cartesian coordinate system, assuming a symmetrical flow field and that flow lines were roughly parallel to the ordinate (hereafter defined as the *y*-direction or the tangential direction) and perpendicular to the abscissa (hereafter defined as the *x*-direction or the radial direction). It was observed that flow lines further away from the cells were non-parallel to the coordinate axes (Fig. 1B); however, in this simple empirical approach we have ignored this fact.

Flow velocities in tangential and radial directions were approximated by an exponential decrease in velocity with decay constants of $-a_t$ and $-a_r$, respectively (Fig. 2). The flow field decayed more rapidly in the radial than in the tangential direction ($a_r > a_t$). Such a velocity field can be rationalized when it is confined by solid boundaries as in microscopic preparations or in interstitial porewaters (Liron & Mochon 1976). Given a cell density of C_v, the mean spacing between cells, termed '*d*' in the following, is equal to $C_v^{-1/3}$. When ciliates are situated in 1 plane, such as in microscopic preparations, it is more convenient to consider the area density, $C_a = d^{-2}$. The radial velocity gradient around a cell is given by $v_x = v_0 \exp(-a_r x)$, where v_0 is the flow velocity at (0,0) (in practice the level of the flow generating ciliary organelles) and x is the radial distance. The total flow (Q) in an equatorial plane around a single cell (Fig. 3A) is then given by:

$$Q = 2\pi v_0 \int_0^\infty x \exp(-a_r x) dx = 2\pi v_0 a_r^{-2} \quad (1)$$

Assuming that, for realistic values of d, almost all flow takes place within a radius of $d/2$ (Fig. 3A), Eq. (1)

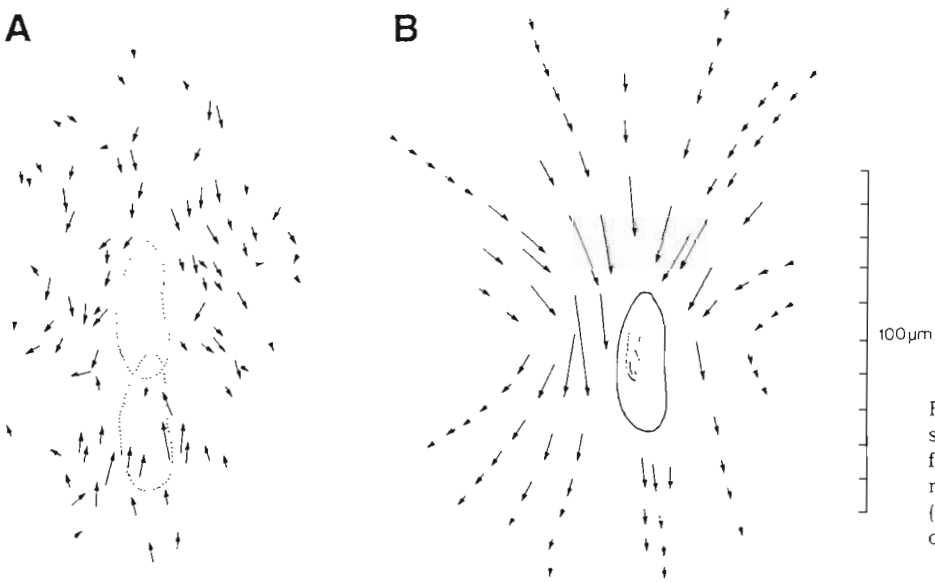

Fig. 1. *Uronema marinum*. Teflon sphere displacements within a time frame of 0.02 s, around (A) a swimming and (B) a feeding *U. marinum*. (A) Dotted lines indicate the outline of the moving ciliate in the 2 consecutive images

can be divided by $2\pi(d/2)^2$ and the mean flow velocity within a radius of $d/2$ can thereby be expressed as:

$$v_x = 8v_0(da_t)^{-2} \quad (2)$$

The tangential flow velocity is given by $v_y = v_x \exp(-a_t y)$, where y is the tangential distance from the equatorial plane; thus $dt/dy = \exp(a_t y)/v_x$ and the time for water to move from $y = 0$ to $d/2$ is given by:

$$T_{(d/2)} = (v_x)^{-1}\int_0^{(d/2)} \exp(a_t y)dy = \frac{1}{a_t v_x[\exp(\frac{1}{2}a_t d)]-1} \quad (3)$$

By substituting the radial velocity v_x with Eq. (2) and noting that the mean tangential velocity from $y = 0$ to $d/2$ can be expressed as $v_y = (d/2)/T_{(d/2)}$, the mean tangential flow velocity in the y-direction within the distance influenced by a single ciliate equals:

$$v_y = \frac{4v_0 a_t}{a_r^2 d[\exp(\frac{1}{2}a_t d)-1]} \quad (4)$$

The transport coefficient (D) within a group of randomly oriented ciliates can be approached as a 2-dimensional random walk with a mean velocity, v_y, between random reorientations and a mean path length 'd' equal to the mean distance between individual ciliates (Fig. 3B):

$$D = v_y(d/4) = \frac{v_0 a_t}{a_r^2[\exp(\frac{1}{2}a_t d)-1]} \quad (5)$$

Microslide experiments. Ciliate suspensions were filled into capillary 'microslides' (Camlab), with internal dimensions of 4.0 × 0.4 mm. The microslides were placed under a microscope and a narrow band of suspended Teflon spheres was injected into the microslide through a microcapillary. The Teflon spheres were 0.8 µm in diameter and close to being neutrally buoyant. Test experiments showed that in the absence of ciliates displacement of spheres was negligible. The spreading of the Teflon spheres caused by the ciliate activity was recorded by the video camera. Fig. 4 shows the spreading of Teflon spheres after injection into a microslide. Distribution of Telfon spheres at given time intervals after injection was quantified by counting the number of spheres within grids placed on a video monitor. Typical spreading distances of the spheres were on the order of 0.5 to 3 mm and only spheres (and cells) in the focal plane (approximately 200 µm) were counted. The distribution of spheres along the injection axis within a ciliate suspension at various times is demonstrated in Fig. 5. Assuming that at any time the spheres were distributed normally along a line perpendicular to the axis of injection (distance 0 in Fig. 5A to E), the spreading of spheres could be approached by a simple diffusion analog by applying the relation: $s^2 = 2Dt$ (Jost 1964), where s is the standard deviation of the particle distribution, t is the time, and D is a transport coefficient for the spheres. A test on subsamples proved to be normally distributed (not shown). Initially the calculated variance (s^2) increased linearly with time (Fig. 5F), and the slope thus a measure of the transport coefficient (D). For the experiment presented in Fig. 5, D was calculated to be 3.7×10^{-5} cm^2 s^{-1} Ciliate densities were calculated

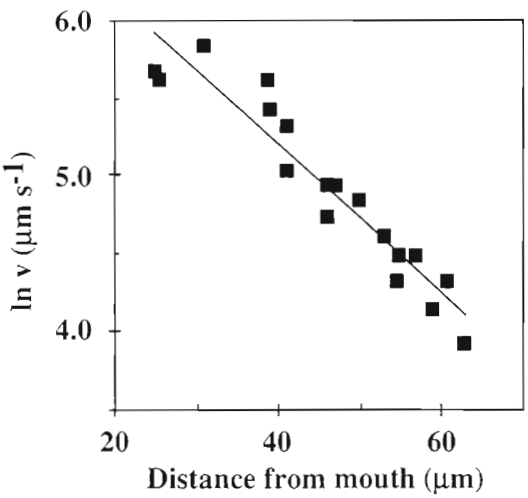

Fig. 2. *Uronema marinum*. The natural logarithm to the tangential flow velocities as a function of the distance to the mouth of a filter feeding *U. marinum*

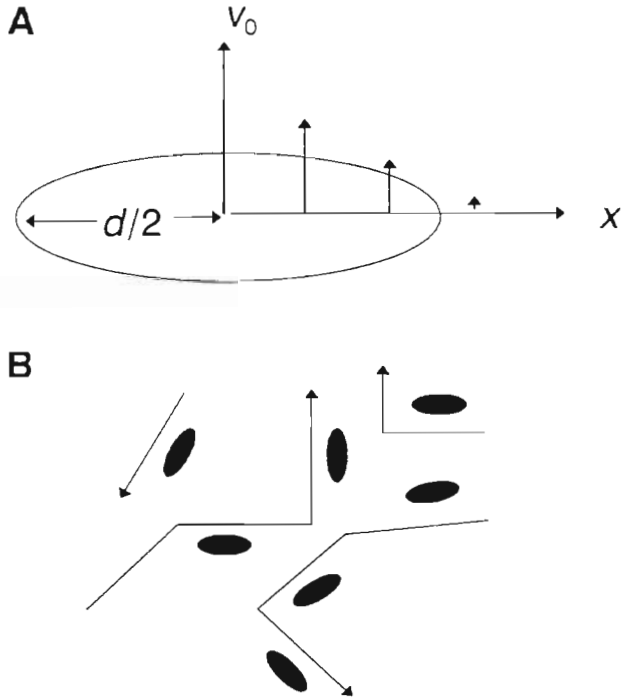

Fig. 3. (A) Schematic presentation of the flow field around a feeding ciliate. d: distance to the nearest neighboring ciliate. (B) A random walk approximation of Teflon beads in a ciliate suspension

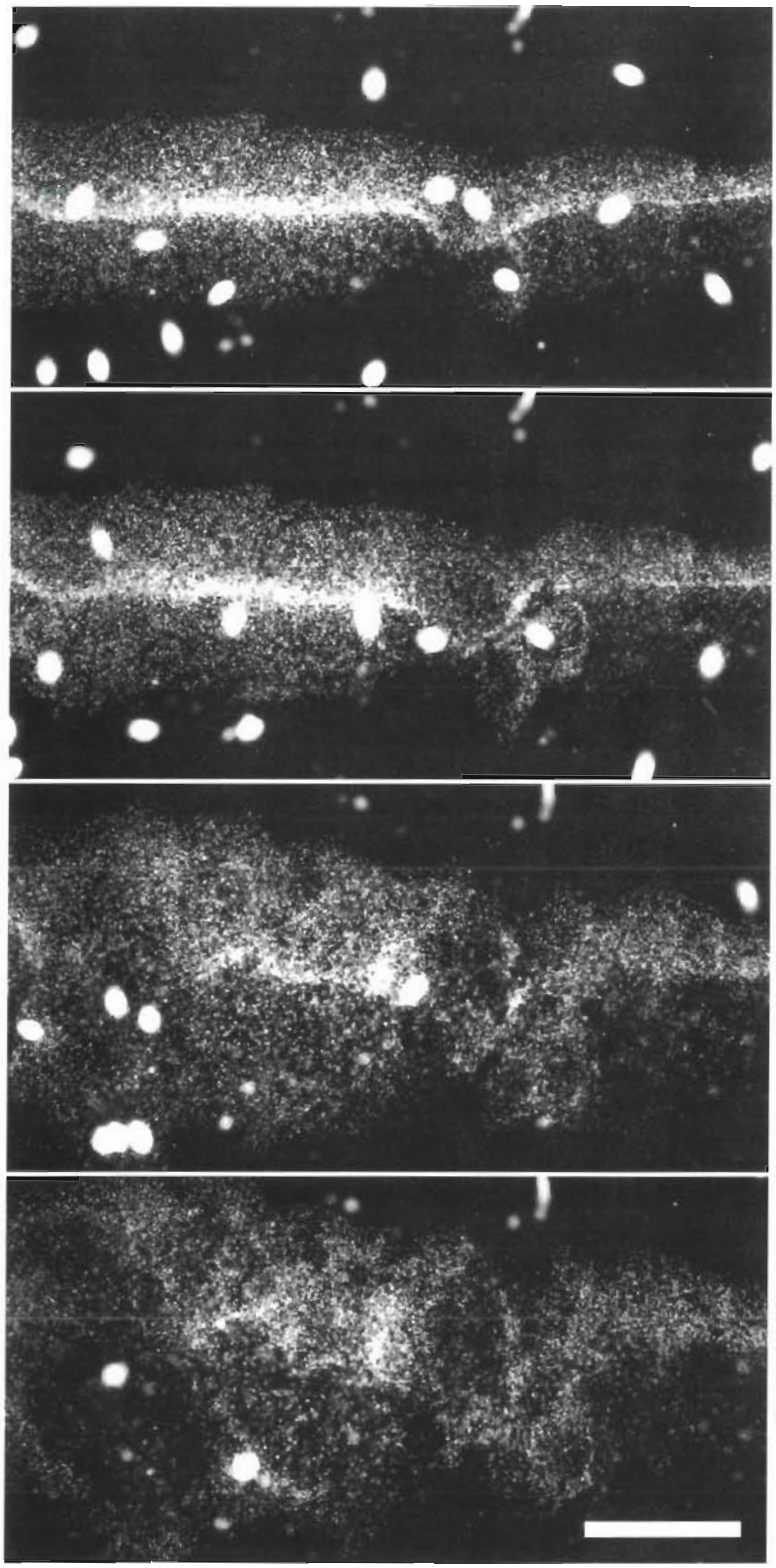

Fig. 4. *Euplotes vannus*. Four photographs taken at 0, 10, 60 and 120 s after injection of Teflon spheres into a microslide. In the first image Teflon spheres are distributed within a narrow band, which on the subsequent images gradually broadens. The individual ciliates (*E. vannus*) can be seen as large white ellipses. Scale bar = 300 µm

from the number of cells recorded during the experiment. *Euplotes* cells did ingest some particles, but the effect of this was negligible.

Chamber experiments. Artificial 'sediments' consisting of glass beads (diameter 2 mm) were sandwiched between 2 well-stirred chambers (Fig. 6). For each experiment, 12 g of glass beads (corresponding to approximately 1100 beads) were added to the chamber resulting in a porosity of 0.30 ± 0.01 within the sediment chamber. The compartments were separated by 5 µm membrane filters with a porosity of approximately 0.70 (Durapore, SVPP). Various densities of ciliates were added to the sediment chamber together with bacteria as a food source. A glass tube connected to the bottom chamber prevented the build-up of pressure gradients during mounting. The complete set-up was allowed to equilibrate for 12 h before Rhodamine WT was added to the upper chamber. In all experiments a volume of 5 µl 20% stock solution of Rhodamine WT (Chrompton & Knowles OT/US 04029NS) was added to the tracer chamber. Rhodamine WT has proven to be an inert, non-adsorbing and stable tracer for flow visualization and is simple to quantify by light absorbance (Huettel et al. 1996). The absorbance was either measured by sampling and subsequent spectrophotometric determination (the 2% dilution per sampling was later corrected for) or was measured on-line via a simple fiber arrangement (Fig. 6). A light-emitting diode (LED) with an emission wavelength of 555 nm was placed on one side of the chamber, while a simple photodiode was placed on the other side. The signal from the photodiode was directly transferred to a strip-chart recorder. The Rhodamine WT was injected into the tracer chamber and after a time lag the absorbance in the measuring chamber increased almost linearly. The rate by which Rhodamine WT passed the measuring chamber was calculated as a function of the ciliate density in the sediment chamber. Typical chamber runs were in the order of 15 to 20 h. After each experiment the porewater from the sediment chamber was sampled and ciliate density was quantified by counting. Cell densities determined before and after the

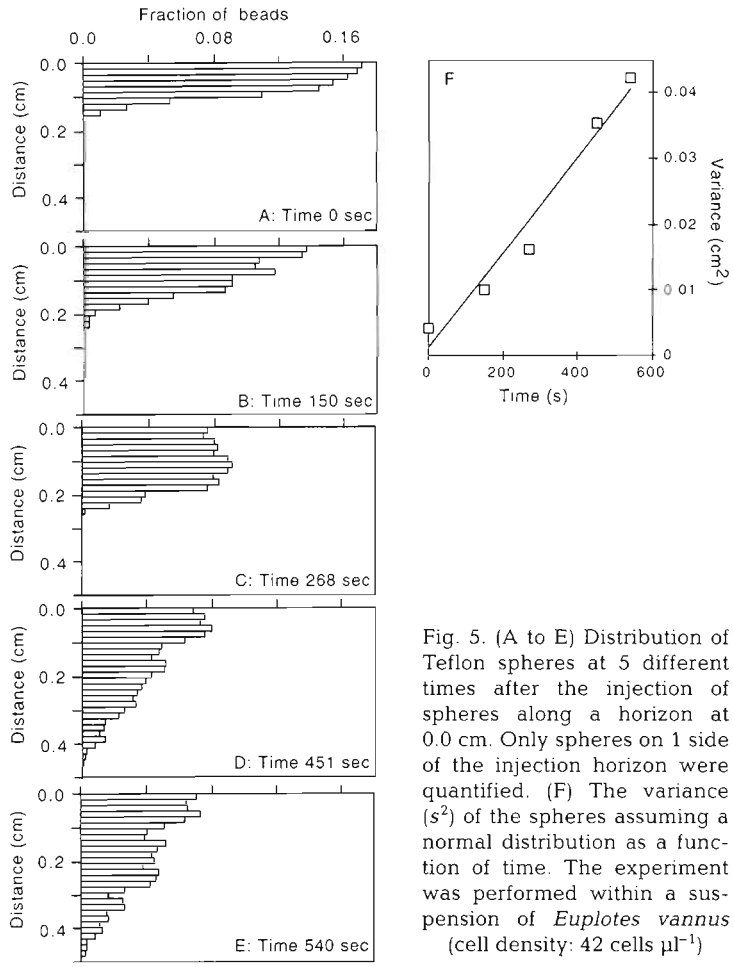

Fig. 5. (A to E) Distribution of Teflon spheres at 5 different times after the injection of spheres along a horizon at 0.0 cm. Only spheres on 1 side of the injection horizon were quantified. (F) The variance (s^2) of the spheres assuming a normal distribution as a function of time. The experiment was performed within a suspension of *Euplotes vannus* (cell density: 42 cells μl^{-1})

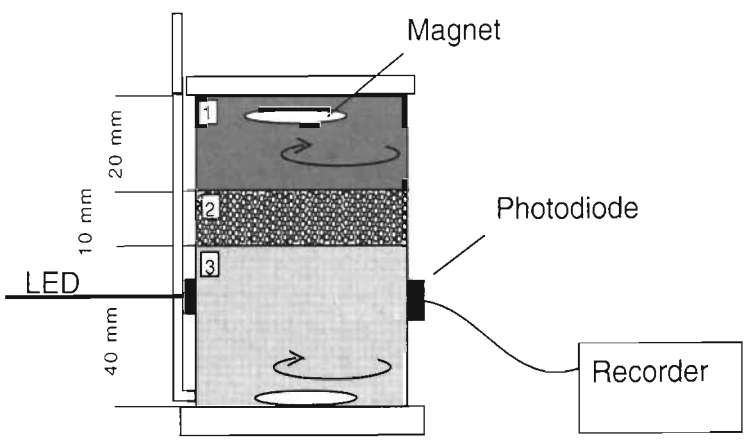

Fig. 6. Schematic drawing of the experimental set-up for the chamber experiments. Compartments 1, 2 and 3 represent the tracer source, the artificial sediment and the measuring chamber, respectively (see 'Materials and methods' for details)

experiments never deviated by more than 8%. All experiments were performed in a thermostated room at 15 ± 1°C.

RESULTS

Initially we recorded the displacement of Teflon spheres around single ciliates. Based on more than 20 flow lines around individuals of *Euplotes* values of v_0, a_t and a_r were estimated to be: 620 $\mu m\ s^{-1}$, 127 cm^{-1} and 315 cm^{-1}, respectively. The corresponding values for *Uronema marinum* were 1160 $\mu m\ s^{-1}$, 468 cm^{-1} and 1392 cm^{-1} Applying these values to Eq. (5) resulted in a empirical relation between cell density and transport coefficients for *Euplotes* and *U. marinum* (Fig. 7). In both instances the transport coefficients increased by several orders of magnitude as the cell density was increased from 100 to 50000 ind. cm^{-2}. Due to the higher filtration rate accomplished by *Euplotes*, the transport coefficient was approximately 1 to 2 orders of magnitude higher than values for *U. marinum* at a given cell density (Fig. 7). Transport coefficients estimated from the spreading of Teflon beads within microslides (see Fig. 5) showed some scatter, but the values generally expressed the same trend as the theoretical approach (Fig. 7).

The rate by which Rhodamine WT was transferred from the tracer chamber to the measuring chamber by pure diffusion (no ciliates present) was $6.2 \times 10^{-3} \pm 2.2 \times 10^{-3}\ h^{-1}$ as inferred from a total of 10 replicate measurements. The addition of *Euplotes* to the porewater at densities of 25 to 304 cm^{-2} increased the transport rate of Rhodamine WT by a factor of up to 2.2 (Table 1). Only 4 experiments were performed with *Uronema marinum*, but all demonstrated a slightly enhanced porewater transport of Rhodamine WT as compared to chambers without ciliates present (Table 1). We do not know the diffusion coefficient of Rhodamine WT. However, if we assume that it is equivalent to the diffusion coefficient of raffinose ($D = 3.2 \times 10^{-6}\ cm^2\ s^{-1}$ at 15°C), which is an organic molecule of the approximate same size as Rhodamine WT (Hayduk & Laudie 1974), the cilate-caused transport coefficients could be estimated (Table 1). For *Euplotes* the estimates generally compared well to the data obtained by the 2 other approaches, while the few *U. marinum* values were somewhat higher (Fig. 7, Table 1).

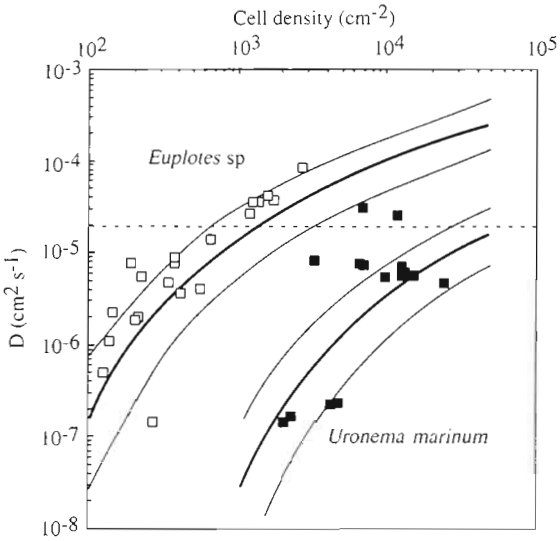

Fig. 7. The transport coefficient (D) as a function of the ciliate density for *Euplotes* and *Uronema marinum*, respectively, calculated from Eq. (5). Thin lines indicate the transport coefficient calculated with a confidence interval of ±20% on each of the 3 parameters V_0, a_t, a_r. The symbols represent experimentally determined transport coefficients from microslide experiments (□: *Euplotes* spp; ■ *Uronema marinum*). (-----) Diffusive coefficient for O_2 at 20°C

DISCUSSION

We applied 3 different approaches in order to demonstrate and quantify the importance of ciliate activity for interstitial solute transport. It was in all instances clear that filter feeding ciliates caused mixing of dissolved material, and we approached the mixing rates by a simple diffusion analogy. Transport coefficients for dissolved material derived from the 3 different approaches agreed reasonably well and, for a given ciliate density, the estimated transport coefficients were, in general, at least within the same order of magnitude.

The physical boundaries experienced by ciliates differed for the 2 experimental approaches. In addition, the theoretical approach assumed a symmetrical flow field, which under normal circumstances would be distorted by the presence of solid surfaces in the vicinity of the ciliates. The effects of distorted flow fields and variable interstitial microgeometry on the transport coefficient are difficult to evaluate; however, the fact that all approaches yielded comparable results indicate that such effects were of minor importance. The frequency and the rate by which ciliates feed are generally independent from the environment or the food concentration (Fenchel 1986). But it may be that the experimental conditions were to a certain degree suboptimal for the ciliates, thus explaining some scatter of the experimental data. Nevertheless, measurements demonstrated increased transport coefficients with increasing ciliate density. Additionally, it was clear that, for a given cell density, the activity of *Euplotes* caused significantly higher transport coefficients than *Uronema marinum*, which has a cell volume that is about 1/20 of that of the *Euplotes* cells.

The diffusion coefficients of important biogeochemical solutes like O_2, NO_3^-, NH_4^+, CO_2 and H_2S are within the range of 1.6 to 2.1 × 10^{-5} cm^2 s^{-1} at 20°C (Broecker & Peng 1974, Boudreau 1997) (at 5°C the values are approximately 40% lower). In order for a population of *Euplotes* spp. to double such transport coefficients cell densities of 700 to 1000 ind. cm^{-2} (corresponding to 19–32 ind. µl^{-1}) would be required, while the density of *Uronema marinum* would have to be 40000 cm^{-2} or 8000 ind. µl^{-1} (Fig. 7). A 10% increase in the oxygen transport coefficient would require an *Euplotes* density of approximately 200 cm^{-2} (3 ind. µl^{-1}) or an *U. marinum* density in the order of 8000 cm^{-2} (700 ind. µl^{-1}).

The natural abundance of ciliated protozoa spans from less than 0.1 µl^{-1} to more than 1000 µl^{-1} (Finlay & Fenchel 1996). Ciliates often accumulate in highly productive niches where the microbial food sources are abundant. Exceptionally high densities are typically encountered in microbial mats. In a study on microbiota in mats of colorless sulfur bacteria the ciliate population, dominated by *Euplotes* and *Uronema* species, reached cell densities of 90 µl^{-1} (Bernard & Fenchel 1995), and *Euplotes* densities as high as 890 µl^{-1} were

Table 1. Ratio between diffusive (D_0) and ciliate stimulated transport coefficient (D) as quantified by the described chamber approach. The calculated values of D are calculated on an estimated diffusive coefficient of Rhodamine WT *Assuming the diffusive coefficient of Rhodamine WT equals that of raffinose at 15°C (3.2 × 10^{-6} cm s^{-1})

Ciliate species	Ciliate density (cm^{-2})	D_0/D	D* (10^{-6} cm^2 s^{-1})
–	0	1	3.2
Euplotes moebiusi	25	0.96	3.1
Euplotes moebiusi	41	1.24	4.0
Euplotes moebiusi	145	1.07	3.4
Euplotes moebiusi	173	1.37	4.4
Euplotes moebiusi	213	1.45	4.6
Euplotes moebiusi	222	1.85	5.9
Euplotes moebiusi	222	2.15	6.8
Euplotes moebiusi	224	1.37	4.4
Euplotes moebiusi	267	1.58	5.0
Euplotes moebiusi	304	2.02	6.4
Uronema marinum	762	1.07	3.4
Uronema marinum	997	1.11	3.5
Uronema marinum	1070	1.51	4.5
Uronema marinum	1525	1.09	3.5

encountered during that study (Bernard & Fenchel unpubl. results). In another study, ciliate populations of cyanobacterial mats were dominated by *E. elegans* and reached cell densities of 5 to 10 μl^{-1} in the upper 2 mm (Fenchel & Bernard 1996). In such communities, the activity of ciliates is likely to be significant for interstitial solute transport; at the most extreme densities mentioned above the diffusive coefficient of O_2 could have been enhanced by a factor of 8 as inferred from Fig. 7. In biofilms or flocks, even higher ciliate densities may be encountered. We measured *Euplotes* densities of 15000 to 20000 cm^{-2} in biofilms that had developed in sediment cores collected at the locality from where the cells were isolated.

Usually the cell density in marine and estuarine sediments is lower, however, and ciliated protozoa often show average densities of 1 to 10 μl^{-1} in the upper cm to mm of such environments (Fenchel 1969, Bak & Nieuwland 1989, Berninger & Epstein 1995). Typically, the highest densities are encountered at the very sediment surface or at the oxic/anoxic interface, which coincides with the horizons with the highest specific O_2 consumption (Berninger & Epstein 1995, Fenchel 1996), and in this zone ciliate filter feeding can be of importance for solute transport. However, in most coastal or shelf sediments the ciliate densities are too low to affect the diffusive mediated solute transport at least for small fast-diffusing molecules such as O_2.

Acknowledgements. We thank Jeanne Johansen for skillful technical assistance during the experiments and Roland Thar and Michael Kühl for help during the development of the online fiber optic measuring system. The study was supported by grants from the Danish Natural Science Research Council (SNF).

LITERATURE CITED

Aller RC, Aller JY (1992) Meiofauna and solute transport in marine muds. Limnol Oceanogr 37:1018–1033

Archer D, Devol A (1992) Benthic oxygen fluxes on the Washington shelf and slope: a comparison of in situ microelectrode and chamber flux measurements. Limnol Oceanogr 37:614–629

Bak RPM, Nieuwland G (1989) Seasonal fluctuations in benthic protozoan populations at different depths in marine sediments. Neth J Sea Res 24:37–44

Bernard C, Fenchel T (1995) Mats of colourless sulphur bacteria. II. Structure, composition of biota and successsional patterns. Mar Ecol Prog Ser 128:171–179

Berninger UG, Epstein SS (1995) Vertical distribution of benthic ciliates in response to oxygen concentration in an intertidal North Sea sediment. Aquat Microb Ecol 9: 229–236

Boudreau B (1997) Diagenetic models and their implementation. Springer-Verlag, Heidelberg

Broecker WS, Peng TH (1974) Gas exchange rates between air and sea. Tellus 26:21–35

Fenchel T (1969) The ecology of marine microbenthos IV. Structure and function of the benthic ecosystem, its chemical and physical factors and the microfauna communities with special reference to ciliated protozoa. Ophelia 6:1–182

Fenchel T (1986) Protozoan filter feeding Prog Protistol 1. 65–113

Fenchel T (1996) Worm burrows and oxic microniches in marine sediments. 2 Distribution patterns of ciliated protozoa. Mar Biol 127:297–301

Fenchel T, Bernard C (1996) Behavioural responses in oxygen gradients of ciliates from microbial mats. Eur J Protistol 32: 55–63

Fenchel T, Glud RN (1998) Veil architecture in a sulphide-oxidizing bacterium enhances countercurrent flux. Nature 394:367–369

Finlay BJ, Fenchel T (1996) Ecology: role of ciliates in the natural environment. In: Hausmann K, Bradbury PC (eds) Ciliates cells as organisms. Gustav Fisher, Stuttgart

Glud RN, Jensen K, Revsbech NP (1995) Diffusivity in surficial sediments and benthic mats determined by use of a combined N_2O-O_2 microsensor. Geochim Cosmochim Acta 59:231–237

Hayduk W, Laudie H (1974) Prediction of diffusion coefficients for nonelectrolytes in dilute aqueous solutions. Am Inst Chem Eng J 20:611–615

Huettel M, Ziebis W, Forster S (1996) Flow-induced uptake of particulate matter in permeable sediments. Limnol Oceanogr 41:309–322

Jost W (1964) Fundamental aspects of diffusion processes. Angew Chem Int Ed Engl 3:713–722

Liron N, Mochon S (1976) Stoke flow for a stokeslet between parallel flat planes. J Engin Math 10:287–303

Purcell EM (1977) Life at low Reynolds number. Am J Phys 45:3–11

Editorial responsibility: Thomas Kiørboe (Contributing Editor), Charlottenlund, Denmark

Submitted: November 30, 1998; Accepted: March 2, 1999
Proofs received from author(s): August 16, 1999